OPEN

# SPECTRAL DOMAIN OPTICAL COHERENCE TOMOGRAPHY FINDINGS IN MACULA-INVOLVING CYTOMEGALOVIRUS RETINITIS

MRINALI P. GUPTA, MD,* SARJU PATEL, MD,* ANTON ORLIN, MD,* ELIZABETH MARLOW, MD,* RU-IK CHEE, MD, MSc,* JENNIFER NADELMANN, BS,† R.V.PAUL CHAN, MD,*‡ DONALD J. D'AMICO, MD,* SZILARD KISS, MD*

**Purpose:** To evaluate the microstructural features of cytomegalovirus (CMV) retinitis by spectral domain optical coherence tomography (OCT).

**Methods:** Subjects were patients with macula-involving CMV retinitis with OCT imaging. The leading edge of retinitis in the macula was identified based on fundus imaging, and OCT findings were longitudinally evaluated in three areas: within the area of active retinitis, at the leading edge of retinitis, and just beyond the leading edge of retinitis.

**Results:** Optical coherence tomography imaging of macular CMV retinitis identified vitreous cells in 10 eyes (100%), posterior vitreous detachment in four eyes (40%), broad-based vitreomacular traction in one eye (10%), epiretinal membrane in eight eyes (80%), and lamellar hole–associated epiretinal proliferation associated with an atrophic hole in one eye (10%). Retinal architectural disruption, disruption of inner retinal layers, disruption of the external limiting membrane, and ellipsoid zone abnormalities were noted within the area of retinitis in all eyes and decreased in frequency and severity at and beyond the leading edge of retinitis, although all 10 eyes (100%) exhibited one of these abnormalities, especially outer retinal microabnormalities, beyond the leading edge of retinitis.

**Conclusion:** Microstructural abnormalities were frequently noted on OCT of CMV retinitis, including within the retina beyond the leading edge of retinitis identified by corresponding fundus imaging. Outer retinal abnormalities were noted more frequently than inner retinal abnormalities beyond the leading edge of retinitis. These findings provide insight into the effects of CMV retinitis on retinal microstructure and potentially on vision and highlight the potential utility of OCT for monitoring microprogression of macula-involving CMV retinitis.

**RETINA** 38:1000–1010, 2018

Cytomegalovirus (CMV) retinitis is a vision-threatening condition that afflicts immunocompromised patients.[1] Although traditionally a condition encountered in patients with human immunodeficiency virus (HIV)/acquired immunodeficiency syndrome, the advent of and advances in antiretroviral therapy have significantly reduced the incidence of CMV retinitis and improved visual outcomes from CMV retinitis in this population.[2–4] Nevertheless, CMV retinitis continues to cause vision loss in patients with HIV.[4,5] Moreover, CMV retinitis also occurs in non–HIV patients including posttransplant patients, especially those on potent immunosuppressive therapy.[5] Cases have also been reported after intraocular or periocular steroid administration in immunocompetent patients.[6,7] Recently, our retrospective study of CMV retinitis from all causes at a tertiary care center found that CMV retinitis remains a vision-threatening problem with risk of vision loss and complications such as retinal detachment.[5]

To date, the microstructural features of active CMV retinitis have not been well characterized in the context of optical coherence tomography (OCT), a modality that we have found clinically useful for monitoring macula-involving CMV retinitis. Various OCT findings such as vitreous debris, vitreous inflammation, retinal architectural disruption, hyperreflective foci, ellipsoid zone (EZ) abnormality, and retinal thickening

or thinning have been reported in a case report fashion (two reports of one case each,[8,9] as well as one case series reporting each of the four individual cases).[10] This study adds to the existing case report literature by evaluating, in a systematic cohort study fashion, the microstructural abnormalities noted on spectral domain (SD) OCT imaging of macula-involving CMV retinitis in distinct zones of retinitis (active retinitis, leading edge of retinitis, and just beyond the leading edge of retinitis), as well as by evaluating how these features evolve over longitudinal follow-up.

## Methods

This is a retrospective, observational cohort study of all patients with newly diagnosed macular CMV retinitis who presented to Weill Cornell Medical College (WCMC) between 2007 and 2015 and had SD-OCT imaging performed. The study protocol was approved by the Institutional Review Board of WCMC, and the study was performed in a manner compliant with the Healthcare Insurance Portability and Accountability Act and the tenets put forth in the Declaration of Helsinki.

The electronic medical record database was queried for all patients with a diagnosis of "CMV retinitis" (*ICD-9* 078.5; *ICD-10* B25.8 and H30.9). The charts of these patients were evaluated to identify patients who met the following inclusion criteria: 1) diagnosis of macula-involving active CMV retinitis based on examination by an experienced retina or uveitis specialist, 2) positive serum or intraocular CMV polymerase chain reaction titers, and 3) SD-OCT imaging available from the time of diagnosis of macular retinitis. The presence of media opacity limiting quality of OCT imaging was an exclusion criterion.

The charts were reviewed to record demographic information, ophthalmic history, and medical history including the cause of immunosuppression and CD4 count (if available). The following ophthalmologic examination details were recorded: best-corrected visual acuity (VA), presence or absence of vitreous detachment, vitreous cell, vitreoretinal interface abnormalities, epiretinal membrane (ERM), cystoid macular edema, and foveal involvement of retinitis. Treatment modalities used during the study period (defined as from the time of diagnosis of macular CMV retinitis until the last available follow-up with SD-OCT imaging available) were recorded, including systemic antiviral therapy, intravitreal antiviral therapy, CMV-specific T-lymphocyte intravenous infusions as previously described,[11] and/or surgery.

Spectral domain OCT volume scans (ranging from $20° \times 15°$ [$5.9 \times 4.4$ mm] with 37 B scans and 123 $\mu$m between B-scan images to $20° \times 25°$ [$6.3 \times 7.8$ mm] with 61 B scans and 131 $\mu$m between B-scan images) obtained using the Heidelberg Spectralis HRA (Heidelberg Retinal Angiograph) + OCT system (Heidelberg Engineering, Inc, Heidelberg, Germany) were reviewed by a retina specialist (M.P.G.). The entire volume scan was evaluated to assess for foveal involvement, foveal cystoid macular edema, vitreous cell, vitreous debris, posterior vitreous detachment (PVD), ERM, and in patients without PVD, subhyaloid hyperreflective deposits. The "largest focus of macular retinitis" and its leading edge were identified from fundus photographs (available in all patients; from the Optos 200Tx [Optos PLC, Dunfermline, Scotland, UK] or Topcon TRC NW8 Fundus Camera [Topcon Medical Systems, Inc., Oakland, NJ]), fundus autofluorescence images (when available; from the Optos 200Tx imaging system), and fluorescein angiographs (when available; from either the Optos 200Tx system or the Heidelberg Spectralis HRA + OCT system). The SD-OCTs were evaluated in three distinct regions relative to this "largest focus of macular retinitis": 1) active retinitis: defined as within the area of active retinitis $>400$ $\mu$m from the leading edge of retinitis; 2) leading edge of retinitis: defined as within the areas of retinitis $<200$ $\mu$m from the leading edge of retinitis; and 3) beyond the leading edge of retinitis: defined as approximately 200 $\mu$m beyond the leading edge of retinitis. In each of these areas, the following OCT features were evaluated: disruption of retinal architecture (defined as none, trace, moderate, or severe); disruption of inner retinal layers (DRILs, defined as the inability to distinguish boundaries between the ganglion cell–inner plexiform layer complex, inner nuclear layer, and outer plexiform layer); presence or absence of cystoid macular edema;

From the *Department of Ophthalmology, Weill Cornell Medical College, New York-Presbyterian Hospital, New York, New York; †Albert Einstein College of Medicine, New York, New York; and ‡Department of Ophthalmology, Illinois Eye & Ear Infirmary, University of Illinois at Chicago, Chicago, Illinois.

This study was funded in part by an unrestricted departmental grant from Research to Prevent Blindness.

S. Kiss has intellectual property related to the use of cytomegalovirus-specific T lymphocytes for the treatment of cytomegalovirus retinitis briefly mentioned in this article. The remaining authors have no financial/conflicting interests to disclose.



Reprint requests: Mrinali P. Gupta, MD, Department of Ophthalmology, Weill Cornell Medical College, 1305 York Avenue, 11th Floor, New York, NY 10065; e-mail: mrp9003@med.cornell.edu

intact or disrupted external limiting membrane (ELM); abnormalities in the EZ (defined as intact, irregular/granular, or absent); presence or absence of hyperreflective intraretinal or subretinal deposits; presence or absence of subretinal fluid; abnormalities in the retinal pigment epithelium (RPE) layer; and overall thickening or thinning of the retina (defined as the area within the boundaries of the internal limiting membrane [ILM] and the RPE).

Statistical analyses were performed using Fisher's exact test for categorical, nonparametric variables and using Student's two-tailed *t*-test for parametric variables (logarithm of the minimum angle of resolution [logMAR] VA), with $P < 0.05$ taken to be significant.

## Results

Of 70 patients identified with a billing diagnosis of CMV retinitis, 10 eyes of 8 patients were included in this study. Sixty-two patients were excluded because of no history of CMV retinitis (11), history of CMV retinitis that was no longer active (33), active CMV retinitis not involving the macula (11), macular CMV retinitis with no available OCT imaging (5), or with media opacity limiting imaging quality (2).

Of the 10 eyes of 8 patients included in this study, mean age at diagnosis of macula-involving CMV retinitis was 43.4 (range 22–56) years, and there was no sex predilection (50% men, 50% women). The underlying immunosuppression was due to HIV/acquired immunodeficiency syndrome in seven eyes (70%) of five patients (62.5%) and due to history of hematologic malignancy status after bone marrow transplant and ongoing immunosuppressant therapy for either graft-versus-host disease prophylaxis or as part of a chemotherapy regimen in three eyes (30%) of three patients (37.5%). CD4 counts were available for 9 of the 10 eyes, with a mean CD4 count of 39.5 (range 0–104) cells/mm$^3$. Mean length of follow-up was 8.0 (range 1.4–17.5) months. During the study period, nine eyes (90%) received systemic antiviral and intravitreal antiviral therapy, and two of these eyes (20% of all eyes in the study) also underwent surgical placement of a ganciclovir implant (Vitrasert; Bausch & Lomb, Rochester, NY). One eye (10%) had previously been treated with multiple systemic and intravitreal antivirals at another institution but during the study period at our institution was treated with intravenous CMV-specific cytotoxic T-lymphocyte infusions alone, with eventual long-term resolution of retinitis as previously reported.[11] At the time of initial diagnosis of macular CMV retinitis, average logMAR VA was 0.33 (Snellen equivalent ~20/43).

Vitreous and vitreoretinal interface abnormalities were frequently noted (Table 1). Vitreous cells were more likely to be identified on OCT imaging (10 eyes, 100%, Figure 1, A and B) than by clinical examination

Table 1. Optical Coherence Tomography Findings in Macula-Involving Cytomegalovirus Retinitis

| Optical Coherence Tomography Finding | No. of Eyes, % |
|---|---|
| Vitreous cells | 10 (100) |
| Vitreous debris | 7 (70) |
| PVD | 4 (40) |
| Vitreomacular traction | 1 (10) |
| ERM | 8 (80) |
| Lamellar hole-associated epiretinal proliferation | 1 (10)* |
| Macular hole | 1 (10) |
| Thickening and hyperreflectivity of retinal vessel walls | 2 (20) |
| Foveal involvement | 6 (60) |
| Cystoid macular edema | 2 (20) |
| Hyperreflective deposits within the retina | 10 (100) |
| ILM separation overlying retinal atrophy and thinning | 8 (80) |

| | Within the Area of Retinitis, n (%) | Leading Edge of Retinitis, n (%) | Beyond the Leading Edge of Retinitis, n (%) |
|---|---|---|---|
| Retinal architecture | | | |
| Normal | 0 | 1 (10) | 2 (20) |
| Trace disruption | 0 | 0 | 6 (60) |
| Mild disruption | 0 | 6 (60) | 2 (20) |
| Severe disruption | 10 (100) | 3 (30) | 0 |
| Disruption of the inner retinal layers | | | |
| No | 0 | 1 (10) | 5 (50) |
| Yes | 10 (100) | 9 (90) | 5 (50) |
| EZ | | | |
| Normal | 0 | 0 | 1 (10) |
| Irregularity/granularity | 0 | 2 (20) | 8 (80) |
| Absent | 10 (100) | 8 (80) | 1 (10) |
| ELM | | | |
| Intact | 0 | 2 (20) | 9 (90) |
| Absent | 10 (100) | 8 (80) | 1 (10) |
| Subretinal hyperreflective deposits | 3 (30) | 4 (40) | 2 (20) |
| Subretinal fluid or hemorrhage | 1 (10) | 3 (30) | 2 (20) |
| Retinal pigment epithelial thickening | 6 (60) | 4 (40) | 2 (20) |

*This patient also had an ERM.

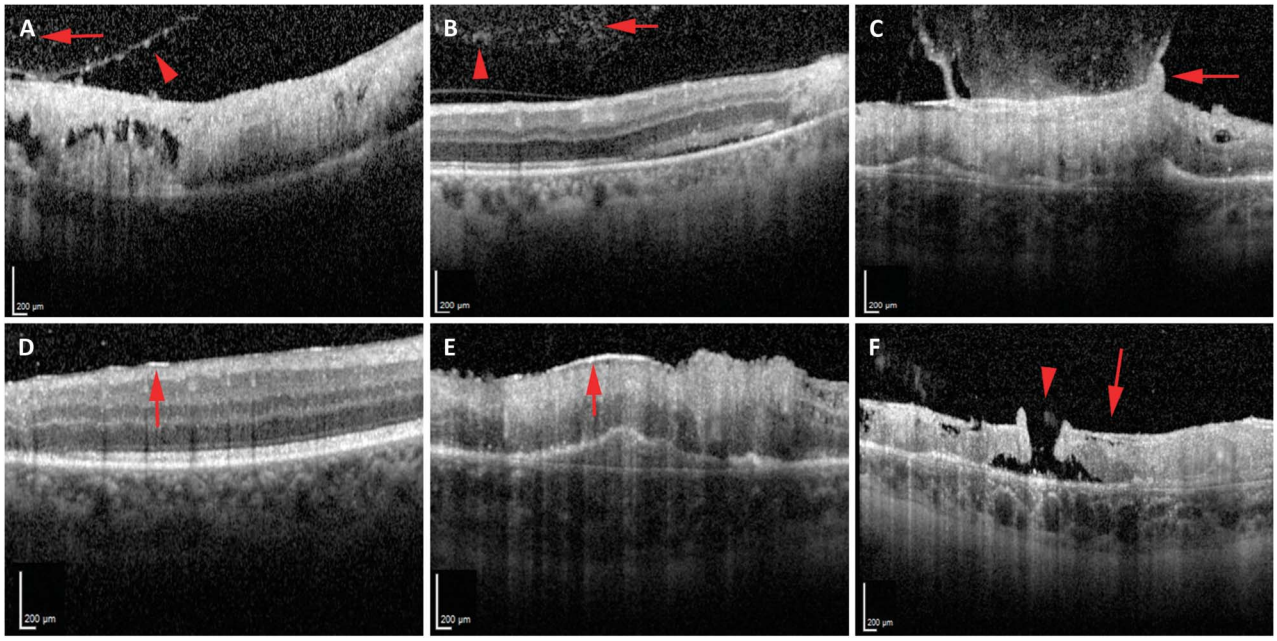


**Fig. 1.** Vitreoretinal interface changes in CMV retinitis. **A** and **B.** Optical coherence tomography identified abnormalities within the posterior vitreous including hyperreflective deposits on the posterior surface of the hyaloid (**A**, red arrowhead), posterior vitreous cells (**A** and **B**, red arrows), and clumps of hyperreflective material consistent with vitreous debris (**B**, red arrowhead). **C–F.** Vitreoretinal interface changes noted on OCT include gliosis of the posterior hyaloid with taut, broad-based vitreomacular traction to the underlying area of retinitis (**C**, red arrow), ERM over retina unaffected (**D**, red arrow) or affected (**E**, red arrow) by retinitis, and a lamellar hole–associated epiretinal proliferation (**F**, red arrow) associated with a full thickness atrophic eccentric macular hole (**F**, red arrowhead) in an area of atrophy from retinitis.

(3 eyes, 30%) ($P$ = 0.003). Vitreous debris was noted on OCT in seven eyes (70%, Figure 1B). Four eyes (40%) exhibited PVD on initial OCT imaging. The incidence of PVD on OCT increased by last follow-up to 9 of 10 eyes (90%). Ultrasound was not performed in any eyes for comparison for presence of vitreous cells, vitreous debris, and/or PVD. One patient exhibited gliosis of the posterior hyaloid with taut, broad-based vitreomacular adhesion and traction over an area of active retinitis (Figure 1C). In eyes without PVD at the time of initial diagnosis, five of the six eyes (83.3%) exhibited hyperreflective deposits on the posterior surface of the hyaloid (Figure 1A). At the time of initial diagnosis of macular CMV retinitis, eight eyes (80%) exhibited some degree of ERM formation, including over retina that was both unaffected (Figure 1D) and affected (Figure 1E) by CMV retinitis. None of these patients were noted to exhibit ERM on clinical examination alone ($P$ = 0.025). All 10 eyes (100%) had ERM on OCT imaging by the last follow-up. In addition to an ERM, one patient also had a separate thicker, medium reflectivity, highly adherent membrane consistent with lamellar hole–associated epiretinal proliferation, which in this case was associated with an eccentric full-thickness macular hole in an area of retinitis and atrophy (Figure 1F and Table 1). This eccentric macular hole did not subsequently enlarge or result in a retinal detachment during the study period.

Optical coherence tomography revealed foveal abnormalities in six eyes (60%) (Table 1). Of these six eyes, five (83.3%) also exhibited foveal involvement on clinical examination, whereas one (16.7%) exhibited no evidence of foveal involvement on clinical examination or on fundus photographs ($P$ = 1.00). Foveal involvement on OCT at presentation was associated with worse VA at presentation (mean logMAR 0.15 [Snellen equivalent ~20/28] with no foveal involvement, mean logMAR 0.44 [Snellen equivalent ~20/55] with foveal involvement; $P$ = 0.036). Final VA was also worse in patients with foveal involvement at diagnosis (mean logMAR 0.97 [Snellen equivalent ~20/187] vs. 0.12 [Snellen equivalent ~20/26]), although this did not reach statistical significance with the small sample size in this study ($P$ = 0.22). Two eyes (20%) had cystoid macular edema on OCT; neither of these patients were noted to have macular edema on examination ($P$ = 0.48). All eyes exhibited hyperreflective spots in the retina (Figure 2, A and B), which variably involved all retinal layers. Two eyes (20%) exhibited thickening and hyperreflectivity of the walls of the retinal vessels consistent with retinal vasculitis (Figure 2A and Table 1).

The retinal architecture was noted to be severely disrupted (see Figure 2C for a representative image of degrees of retinal architecture disruption) within the area of active retinitis in all 10 eyes at diagnosis,

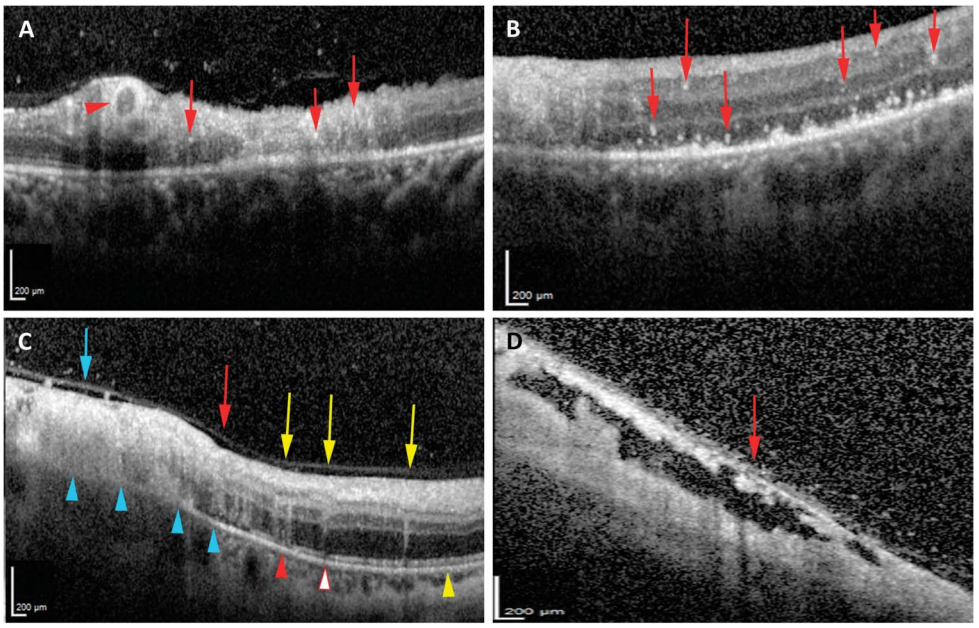


**Fig. 2.** Intraretinal abnormalities on OCT imaging of CMV retinitis. **A** and **B.** Optical coherence tomography imaging of CMV retinitis demonstrated hyperreflective inner retinal deposits in variable retinal layers (**A** and **B**, red arrows), as well as hyperreflectivity and thickening of the retinal vasculature (**A**, red arrowhead) consistent with retinal vasculitis. **C.** Representative image showing variable retinal architecture disruption and EZ abnormalities on OCT imaging ranging from severe disruption of the retinal layers, in which none of the layers are discernible (blue arrow), moderate disruption of the retinal architecture (red arrow), in which some of the retinal layers are obscured, and trace disruption of the retinal architecture, characterized by subtle "smearing" of the retinal layers (yellow arrow). While all areas of severe and moderate retinal architectural disruption exhibit disruption of the inner retinal layers (blue and red arrows), inner retinal layers remained intact in some areas with trace retinal architectural disruption (yellow arrows). Ellipsoid zone abnormalities ranged from absence of the EZ (blue arrowhead), irregularity or granularity of the EZ (red arrowhead and red outlined arrowhead), or intact (yellow arrowhead) EZ. External limiting membrane was absent in all of absent EZ (blue arrowheads), either intact (red outlined arrowhead) or absent (red arrowhead) where EZ was irregular, and intact in all areas where EZ was intact (yellow arrowhead). **D.** Internal limiting membrane separation was noted in some cases overlying areas of retinal atrophy (red arrow).

and the degree of retinal architectural disruption decreased at and beyond the leading edge of retinitis (Table 1). Evidence of some degree of retinal architectural disruption was noted in the retina beyond the leading edge of retinitis in 8 of the 10 eyes (80%). Disruption of the inner retinal layer (Figure 2C) likewise was noted in all eyes (100%) within the area of active retinitis, and its frequency decreased at the leading edge and beyond (Table 1). All areas with moderate to severe retinal architecture disruption also exhibited DRIL. Of the areas with trace retinal architecture disruption (all within the area just beyond the leading edge of retinitis), only 50% also exhibited DRIL (Figure 2C). Over time, the retinal architecture worsened such that at the leading edge of retinitis, nine eyes (90%) exhibited severe disruption of the retinal layers by the final follow-up, and in the area just beyond the leading edge, three eyes (30%) exhibited severe disruption of the retinal layers. In addition, two of the three eyes (66.7%) initially with trace retinal architecture disruption and DRIL exhibited worsening of the retinal architecture over time, whereas 0 of the three eyes (0%) with trace architectural disruption without DRIL exhibited overall worsening of retinal architecture. However, the association of DRIL with longitudinal worsening retinal architecture did not achieve statistical significance ($P = 0.40$). Within the area of active retinitis, there was noted to be one or more areas of preserved and detached ILM overlying atrophic retinal changes in eight eyes (80%, Figure 2D and Table 1).

The EZ was absent on OCT in the area of active retinitis in all 10 eyes (100%; see Figure 2C for representative images of degrees of EZ disruption). The degree and frequency of EZ abnormalities decreased at and beyond the leading edge of retinitis (Table 1). At leading edge of active retinitis, all 10 eyes (100%) had EZ abnormalities, with 8 eyes (80%) showing absence of the EZ and 2 eyes (20%) showing irregularity and/or granularity of the EZ. In the retina just beyond the leading edge of retinitis, the EZ was intact in only one eye (10%), whereas eight eyes (80%) exhibited irregularity and granularity, and one eye (10%) exhibited absence of the EZ (Table 1). At initial diagnosis, ELM disruption was noted in all 10 eyes (100%) in the area of active retinitis, in 8 of the 10 eyes (80%) at the leading edge, and in 1 of the 10 eyes (10%) at the area beyond the leading edge of retinitis (Table 1 and Figure 2C). External limiting membrane disruption was associated with worse EZ features (ELM was disrupted in 0 of the 1 retinal area with normal EZ [0%], in 2 of the 10 retinal areas with irregular EZ [20%], and in 19 of the 19 areas with absent EZ [100%], $P < 0.001$). Overall, the EZ abnormalities persisted or worsened through the last follow-up in all 10 eyes in each of the 3 areas studied (i.e., in all 30 locations studied) except in 1 eye in the area beyond the leading edge of

retinitis, where the EZ had initially been irregular but subsequently normalized by the last follow-up. In this eye, the ELM was initially intact in the area where the EZ eventually normalized.

Figure 3 is a representative case demonstrating fundus photographs with the three discrete zones (active retinitis, leading edge of retinitis, and beyond the leading edge of retinitis) noted (Figure 3A). Fundus autofluorescent imaging (Figure 3B) shows hypo- and hyperautofluorescence in the area of active retinitis with a hyperautofluorescent border and a subtle surrounding hyperfluorescence, the boundaries of which are not clearly evident. Optical coherence tomography imaging through the three zones of retinitis exhibit microstructural abnormalities that are worst in the area of retinitis and least notable in the area beyond the leading edge of retinitis (Figure 3, C–E).

We noted that identification of the boundary of EZ abnormality on OCT may be useful for tracking progression or stability of CMV retinitis. The location marker in the Heidelberg Spectralis viewing system was placed at the border of normal and abnormal EZ at initial OCT and referenced for longitudinal comparison. In well-controlled CMV retinitis, the EZ abnormalities did not progress beyond the marker. Over time, additional retinal abnormalities, most notably further destruction of retinal architecture and retinal thinning were noted in the retina overlying affected, abnormal EZ, whereas the retina overlying normal EZ remained stable. With progressive CMV retinitis, the border of abnormal EZ progressed farther into the area of previously normal appearing retina and EZ. Two representative cases are shown here (Figure 4). Case one is a 56-year-old man with HIV/acquired immunodeficiency syndrome (CD4 count 27 cell/mm$^3$) and a history of lymphoma in remission after chemotherapy who was diagnosed with macula-involving CMV retinitis in the right eye for which he was started on systemic oral valganciclovir and intravitreal antivirals. On follow-up 10 days later, the retinitis had progressed clinically, which was evident on OCT by extension of the boundary of abnormal EZ, as well as worsening overlying intraretinal involvement (Figure 4A). Therapy was escalated and achieved control of CMV retinitis, such that on OCT imaging 2 months later (Figure 4B), the boundary of abnormal and normal EZ remained stable and the retina overlying the area of abnormal EZ demonstrated progressive retinal thinning. The retina overlying the

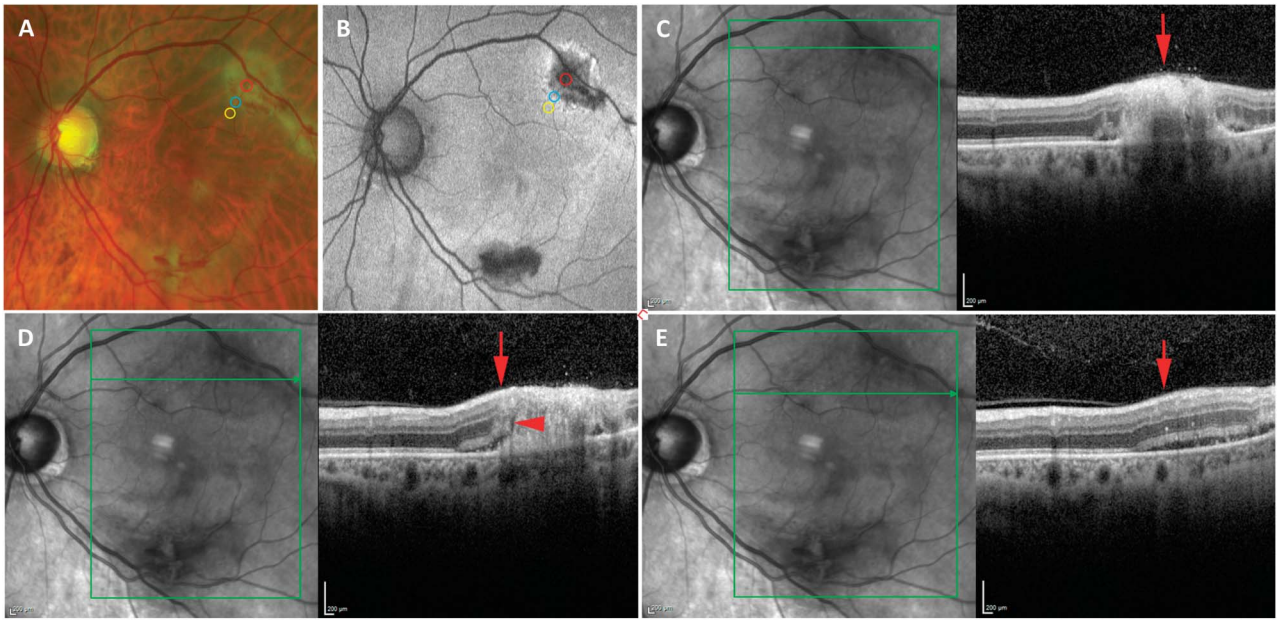


**Fig. 3.** Imaging of a representative case of CMV retinitis showing OCT findings in areas of active retinitis, the leading edge of retinitis, and beyond the leading edge of retinitis noted on fundus photographs. **A.** Fundus photographs of a case of macular CMV retinitis in the left eye in which the largest focus was over the superior arcades with retinal whitening and hemorrhage. The area of active retinitis (red circle), leading edge of retinitis (blue circle), and area of retina just beyond the leading edge (yellow circle) are noted. **B.** Fundus autofluorescence imaging of the same patient showed hypo- and hyperautofluorescence in the areas of active retinitis with a hyperautofluorescent border at the leading edge, the boundaries of which are not clearly evident. The area of active retinitis (red circle), leading edge of retinitis (blue circle), and area of retina just beyond the leading edge (yellow circle) are noted. **C**–**E.** Optical coherence tomography imaging through the area of active retinitis (**C**), leading edge of retinitis (**D**), and beyond the leading edge of retinitis (**E**) reveal microstructural abnormalities. (**C**) The area of active retinitis (red arrow) reveals severe retinal architectural disruption and obliteration of the EZ and ELM. **D.** The leading edge (red arrow) reveals moderate retinal architectural disruption with thickening and irregularity of the EZ (red arrowhead), absence of the ELM (red arrowhead), and subretinal fluid and hyperreflective subretinal deposits (red arrowhead). **E.** The area beyond the leading edge of retinitis (red arrow) reveals relatively intact retinal architecture but a few intraretinal hyperreflective foci, thickening and irregularity of the EZ, intact ELM, and subretinal fluid and hyperreflective deposits.

unaffected EZ retained its architecture and thickness (Figure 4B). Case two is a patient in whom CMV retinitis control was achieved initially, with no interval change in the boundary of normal and abnormal EZ from the time of diagnosis to 17.5 months later. Again, there was progressive retinal thinning of the retina overlying the abnormal EZ, whereas the retina overlying intact EZ remained normal (Figure 4C).

Subretinal hyperreflective deposits were noted in the area of active retinitis in three eyes (30%), at the leading edge in four eyes (40%), and beyond the leading edge in two eyes (20%). Subretinal fluid or hemorrhage was noted in the area of active retinitis in one eye (10%), at the leading edge in three eyes (30%), and beyond the leading edge in two eyes (20%). Retinal pigment epithelium thickening was noted in the area of active retinitis in six eyes (60%), at the leading edge in four eyes (40%), and beyond the leading edge in two eyes (20%) (Table 1).

Overall, 10 eyes (100%) exhibited one or more abnormalities on OCT in the retina just beyond the leading edge of retinitis. By last follow-up, two of these eyes (20%) exhibited normal retinal microstructure on OCT in this area, whereas 8 (80%) exhibited some degree of retinal architecture disruption (3 eyes [30%] with severe disruption) and EZ abnormalities. Five of those eight eyes also exhibited retinal thinning in this area.

## Discussion

Despite advances in antiretroviral therapy for patients with HIV and a corresponding reduction in the

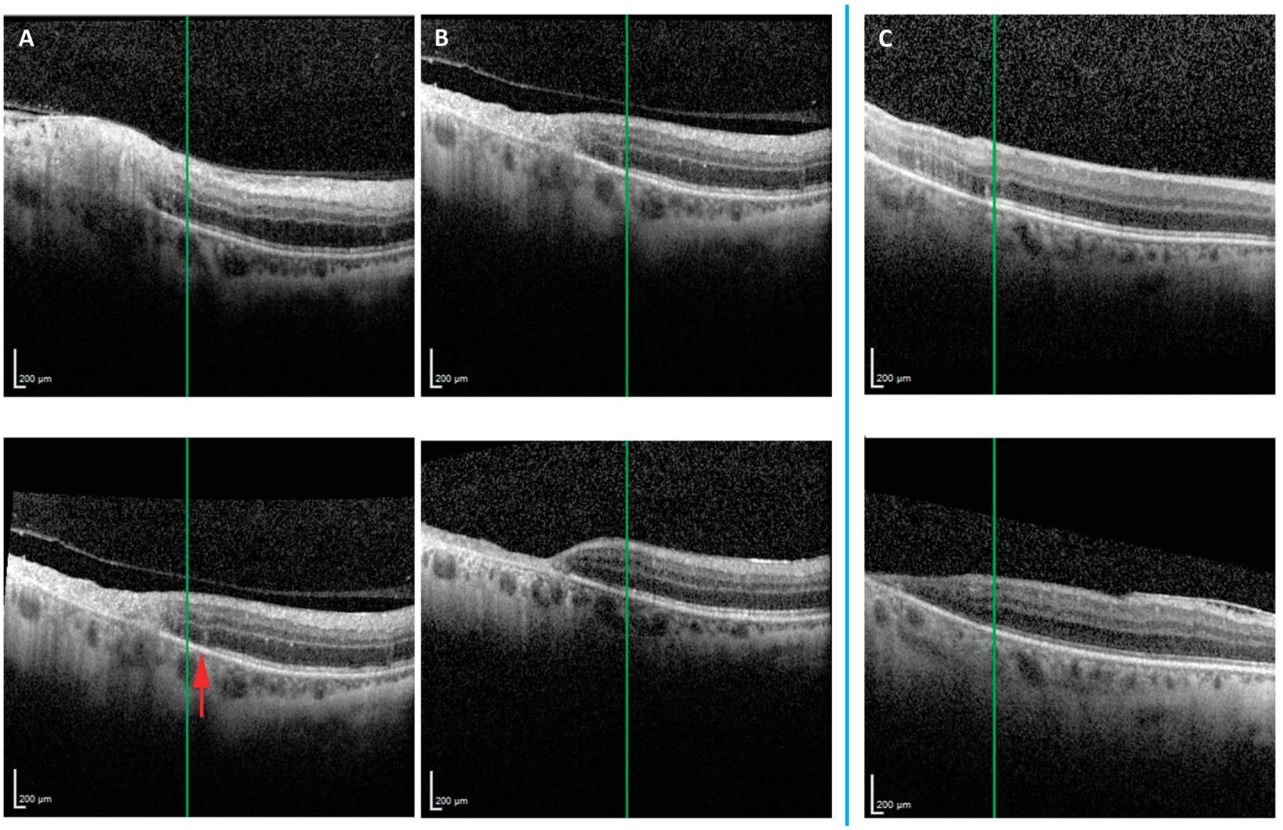


**Fig. 4.** The boundary of EZ abnormality was monitored longitudinally to assess for progression or stability at the leading edge of macular CMV retinitis (**A**–**C**). Case 1 (**A** and **B**) is a patient who had OCT evidence of macular CMV retinitis with retinal architecture disruption and EZ abnormalities (the boundary of which is denoted by the green line marker) at presentation (**A**, top panel). At follow-up 10 days later, the CMV retinitis had progressed clinically, and OCT (**A**, bottom panel) showed progressive retinal thinning in the area of previously noted retinitis, as well as new areas of trace disruption of the retinal architecture and new areas of EZ disruption (red arrow; loss of EZ to the right of the green line marker). Therapy was escalated and achieved control of CMV retinitis clinically, which was also noted on OCT as no progression of the EZ abnormality from that time point (**B**, top panel; green line marker with EZ disruption to the left and intact EZ to the right) until follow-up 2 months later (**B**, bottom panel; green line marker continues to show disrupted EZ to the left and stable intact EZ to the right). The retina overlying abnormal EZ (**B**, top and bottom panels, left side of green line marker) demonstrated mild retinal thinning, whereas the retina overlying unaffected EZ (**B**, top and bottom panels, right side of green line marker) retained its architecture and thickness over time. Case two demonstrates a patient with well-controlled CMV retinitis, in whom follow-up OCT (**C**, bottom panel) 17.5 months after initial diagnosis (**C**, top panel) showed no progression of the EZ abnormalities (the border of which is denoted by the green line marker). There was progressive disruption of the retinal architecture and thinning of the retina in the retina overlying abnormal EZ (**C**, top and bottom panels, left side of green marker), but not in the retina overlying the unaffected EZ (**C**, top and bottom panels, right side of green marker).

incidence of CMV retinitis and its consequent visual morbidity, CMV retinitis continues to cause vision loss in patients.[4,5] Previously, although OCT features of CMV retinitis have been reported in a case report fashion,[8–10] yet no study has systematically evaluated this topic. In this retrospective cohort study, we evaluated microstructural features on OCT imaging in the area of active retinitis, at the leading edge of active retinitis, and in retina just beyond the leading edge of retinitis, as determined by fundus photographs. We noted a high frequency of vitreoretinal and intraretinal abnormalities that could affect vision. Our description of these abnormalities may serve to shed light onto the effects of CMV on the retinal microstructure and accordingly on vision, as well as highlight the potential utility of OCT for monitoring macular CMV retinitis.

Cytomegalovirus retinitis is classically thought to impact vision when the retinitis affects the nerve or fovea, or when a retinal detachment occurs secondarily. In this study, we found several vitreoretinal interface abnormalities on OCT that can affect vision. One eye (10%) exhibited broad-based vitreomacular traction from an area of gliotic, thickened hyaloid that was highly adherent to an area of active retinitis. Eight of the 10 eyes (80%) in this study exhibited ERM at the time of initial diagnosis of macular retinitis, and all 10 (100%) eyes had ERM by last follow-up. Previous studies have noted a similar frequency of ERMs in patients with healed, inactive macular retinitis,[12] and one case report previously noted an ERM in the setting of active macular CMV retinitis.[9] Our study suggests that these ERMs may frequently be present early in the disease course.

A major mechanism for idiopathic ERM formation implicates PVD, in which either cortical vitreous remnants are left behind and proliferate or in which ILM breaks occur and subsequently allow cells to migrate to the inner retinal surface. Secondary ERM formation in inflammatory ocular disease is thought to be mediated by cytokines that promote proliferation of not only glial cells typically found in idiopathic ERMs but also leukocytes.[13] In this study, an inflammatory etiology is suggested by the relative higher frequency of ERMs (8 of the 10 eyes) than PVD (4 of the 10 eyes) at diagnosis, as well as the frequent identification of posterior vitreous cells on OCT and of hyperreflective deposits (which may represent cellular debris) on the posterior hyaloid surface of eyes without PVD. Vitreous cells were noted more frequently on OCT (10 eyes [100%]) than on examination (3 eyes [30%]) ($P = 0.003$). This may reflect the posterior localization of the vitreous cells identified on OCT, as compared to the anterior slit-beam assessment of vitreous cells during examination, or the superior resolution of OCT imaging. Previous case reports have also noted vitreous cells or debris on OCT imaging of CMV retinitis.[9] Although only four eyes (40%) had PVD at diagnosis of CMV retinitis, nine eyes (90%) had PVD by the last follow-up. It is unclear whether the increase in PVD rates over time is related to vitreoretinal interface changes secondary to retinitis or inflammation or to the frequent intravitreal injections administered for treatment.

In addition to ERMs, one patient also exhibited a medium reflectivity, thick, highly adherent membrane with features similar to lamellar hole–associated epiretinal proliferation (LHEP), which is thought to be a distinct entity from conventional ERM. Although LHEP is most commonly associated with lamellar holes, it is also seen in the setting of full-thickness macular holes. Although the pathogenesis of LHEP is still being investigated, it is currently thought that LHEP is driven by proliferation of Müller cells from the exposed middle retinal layers of the macular hole onto the inner retina. Thus, it is thought that the LHEP may be a response to hole formation rather than a cause—that is, the LHEP is not thought to exert traction contributing to hole formation.[14–16] Consistent with this hypothesis, the LHEP identified in this study was found in association with an eccentric macular hole in an area of retinitis that presumably occurred secondary to atrophy from CMV retinitis rather LHEP-induced traction.

Optical coherence tomography may suggest prognosis for VA if it were able to identify foveal involvement better than clinical examination or other imaging. In this study, foveal involvement by OCT at initial diagnosis was noted in six eyes (60%) and correlated, as expected, with worse VA at presentation (logMAR 0.44 vs. logMAR 0.15, $P = 0.036$) and exhibited a trend toward worse final VA (logMAR 0.97 vs. logMAR 0.12, $P = 0.22$). However, clinical examination had also identified foveal involvement in five of the six eyes with foveal involvement on OCT. Thus, it is unclear from this small study whether OCT may prove useful on this front.

In this study, we identified a number of retinal microstructural abnormalities from CMV retinitis. The hallmark feature was marked disruption of the retinal architecture which was most severe in the area of active retinitis and decreased in severity at and beyond the leading edge of retinitis. Even beyond the leading edge of retinitis, OCT revealed some retinal architectural disruption. Case reports have also previously reported retinal architecture disruption on OCT in CMV retinitis.[9,10] Although DRIL was noted in all cases with moderate or severe retinal architectural

disruption, we did note that 50% of eyes with trace architectural disruption exhibited no DRIL. The retinal architectural abnormalities in these eyes primarily involved middle and outer retinal layers, suggesting that the outer retina may be affected earlier on in CMV retinitis. Previous studies in other disease states such as diabetic macular edema have suggested that DRIL can be an imaging marker for VA and that change in DRIL can be a marker for change in VA.[17] The impact of retinal architecture disruption and DRIL in this study on vision is unclear as most cases involved nonfoveal CMV retinitis. However, eyes with only trace retinal architectural disruption but evidence of DRIL were more likely to exhibit worsening of the retinal architecture over time, although this did not achieve significance, possibly because of the small sample size.

Eight eyes (80%) in this study revealed areas of ILM separation over areas of retinal atrophy, as if the ILM initially remained intact while the underlying retina atrophied. Previous studies have suggested that although CMV does infect Müller cells,[18–20] they may be more resistant to infection than other retinal and retinal vascular tissues.[19,20] This relative resistance to infection may explain why the ILM, formed by footpads of the Müller cells, initially remained intact even when the underlying retina underwent necrosis.

Ellipsoid zone abnormalities, also noted previously in two previous case reports,[9,10] were universally present in areas of active retinitis and decreased in frequency and severity at and beyond the leading edge of active retinitis, although there was a high frequency (90%) of EZ abnormalities beyond the leading edge of retinitis. Although ELM disruption was also noted in all eyes within the area of active retinitis, it was infrequently noted (10%) beyond the leading edge of retinitis. Moreover, ELM disruption correlated to worse EZ features and was universally noted in cases with absent EZ, infrequently noted in areas with milder EZ abnormalities, and never noted in areas of intact EZ. These findings suggest that ELM disruption may occur later in CMV retinitis than EZ changes and are consistent with other studies suggesting that disorganization in the ELM is a later effect than EZ disruption in photoreceptor damage.[21–23] Studies in other disease states also suggest that photoreceptor restoration occurs in the opposite direction (with EZ recovery occurring later than ELM recovery)[24]; however, only one of the 30 evaluated retinal areas in this study exhibited recovery of the EZ (and this eye had baseline intact ELM). Finally, although abnormalities in the EZ and ELM have been correlated to reduced VA in a multiple other retinal diseases,[25–28] the infrequency of foveal-involving macular CMV retinitis in this study precluded the ability to correlate these features to VA.

A previous case series reported a halo of hyperautofluorescence at the leading edge of clinically evident CMV retinitis and suggested that increased engulfment of cellular and photoreceptor debris by RPE and/or microglia in this area may be responsible.[29] Our findings of EZ and ELM disruption as well as accumulation of subretinal hyperreflective deposits that may contain fluorophores (4 eyes, 40%) and RPE thickening (4 eyes, 40%) at the leading edge of retinitis lend further support to the theory that a pathologic process involving increased phagocytosis of photoreceptor cellular debris may be occurring at the leading edge of retinitis.

Several findings in this study suggest that the outer retinal tissues may be affected earlier than inner retinal tissues in the course of CMV retinitis. We noted a high frequency of outer retinal (EZ and ELM) abnormalities at and beyond the leading edge of retinitis. In addition, we noted cases beyond the leading edge of retinitis that exhibited no DRIL but had trace architectural disruption primarily involving the middle and outer retinal layers. Although only 50% of eyes had DRIL beyond the leading edge of retinitis, 90% exhibited EZ abnormalities. The susceptibility of outer retinal tissues to CMV virus is supported by the aforementioned case series reporting autofluorescence abnormalities in the retina beyond the leading edge of retinitis,[29] as well as by a mouse model study in which CMV virions were injected into the supraciliary body of immunosuppressed mice.[19] The retinitis was noted to affect the RPE and photoreceptors early on, with subsequent damage to the inner retinal neural tissues and Müller cells. It should be noted, however, that although the findings of this description study are suggestive of earlier damage to the outer retina from CMV retinitis, it is not possible to assess whether these microstructural abnormalities are due earlier spread of virus particles to the outer retina or due to increased susceptibility of these outer retinal tissues to penumbra effects such as inflammation from adjacent infectious retinitis. Overall, in this study, 10 eyes (100%) exhibited one or more abnormalities on OCT in the retina beyond the leading edge of retinitis. By the last follow-up, two eyes (20%) exhibited normalization of the microanatomy, suggesting that there may be a penumbra effect in at least some cases. For the eight eyes (80%) with persistent retinal microstructural abnormalities, it is unclear if the retinal abnormalities were due to progressive damage to the retina already affected at the time of diagnosis or if the retinitis had progressed. Further studies with more patients are needed to evaluate this further.

The frequent identification of microstructural abnormalities on OCT in areas of retina beyond the leading edge of retinitis identified by fundus photography suggests that the detailed microscopic resolution afforded by OCT may allow better determination of the precise boundary of involvement. This may, in turn, improve detection of microscopic progression. Among all the abnormalities noted on OCT in this study, we noted that the sharpest identifiable boundary between normal and abnormal microstructure was at the junction of normal and abnormal (irregular or absent) EZ. Moreover, as noted above, our study and other studies[19] suggest that EZ disruption may be an early microstructural abnormality in CMV retinitis. Monitoring the boundary of EZ involvement on OCT over sequential visits may be helpful in identifying stable versus progressing cases. We propose that if the CMV retinitis remains controlled, the transition between normal and abnormal EZ remains stable. If CMV retinitis progresses clinically, the boundary of normal and abnormal EZ advances. In addition, over time, the retina overlying abnormal EZ develops progressive microstructural abnormalities including disruption of the retinal architecture and thinning, whereas the retina overlying normal EZ retains normal architecture. Although CMV retinitis progresses slowly in most cases, micrometers of progression can have significant impact of vision in retinitis threatening the nerve or fovea. Moreover, earlier detection of progression may allow earlier escalation of or changes in therapy. Thus, the use of OCT to monitor for microprogression may have clinical utility, although such an analysis was beyond the scope of this descriptive study. Further studies are necessary to evaluate the utility of OCT imaging in general and OCT EZ abnormalities in particular for monitoring CMV retinitis, especially in comparison with clinical examination and other imaging modalities such as fundus photos or autofluorescence.

This study has several limitations, including its retrospective, observational nature and the small number of cases included. In addition, because of the retrospective nature, boundaries of active retinitis were identified by fundus photographs and (when available) additional imaging. There are no data on the accuracy and precision of retinitis boundary assessment from fundus photographs; however, the extent of retinitis noted on clinical examination could not be determined retrospectively. Still, many previous studies evaluating CMV retinitis progression rates have used fundus photography. Comparison of OCT imaging with clinical examination may nevertheless be more clinically relevant, and future studies may evaluate this further. The retrospective nature and absence of a gold standard to identify progression versus stability (e.g., aqueous CMV viral load) similarly precluded the ability in most cases to determine whether changes over time were due to evolution of the disease itself or progression of retinitis. Correlation with fundus autofluorescence would have been instructive; however, autofluorescence imaging was not available for several subjects in this already small sample size study. Finally, this study is descriptive and, therefore, was not designed to evaluate whether or how OCT imaging can change management of CMV retinitis. Further studies are necessary to this end.

**Key words:** cytomegalovirus retinitis, optical coherence tomography, ellipsoid zone, external limiting membrane, disruption of the inner retinal layers.

## References

1. Carmichael A. Cytomegalovirus and the eye. Eye 2012;26: 237–240.
2. Hoover DR, Peng Y, Saah A, et al. Occurrence of cytomegalovirus retinitis after human immunodeficiency virus immunosuppression. Arch Ophthalmol 1996;114:821–827.
3. Sugar EA, Jabs DA, Ahuja A, et al. Incidence of cytomegalovirus retinitis in the era of highly active antiretroviral therapy. Am J Ophthalmol 2012;153:1016–1024.
4. Jabs DA, Ahuja A, Van Natta ML, et al. Long-term outcomes of cytomegalovirus retinitis in the era of modern anti-retroviral therapy: results from a United State Cohort. Ophthalmology 2015;122:1452–1463.
5. Orlin A, Nadelman J, Gupta MP, et al. Cytomegalovirus retinitis in the era of antiretroviral therapy at a tertiary care center. J Vitreoretin Dis. 2017;1:57–64.
6. Ufret-Vincenty RL, Singh RP, Lowder CY, et al. Cytomegalovurs retinitis after fluocinolone acetonide (Reticert) implant. Am J Ophthalmol 2007;143:334–335.
7. Takakura A, Tessler HH, Goldstein DA, et al. Viral retinitis following intraocular or periocular corticosteroid administration: a case series and comprehensive review of the literature. Ocul Immunol Inflamm 2014;22:175–182.
8. Giano A, Sabella P, Eandi CM, et al. Spectral-domain optical coherence tomography findings in a case of frosted branch angiitis. Eye 2010;24:941–943.
9. Kurup SP, Khan S, Gill MK. Spectral domain optical coherence tomography in the evaluation and management of infectious retinitis. Retina 2014;34:2233–2241.
10. Arichika S, Uji A, Yoshimura N. Retinal structural features of cytomegalovirus retinitis with acquired immunodeficiency syndrome: an adaptive optics imaging and optical coherence tomography study. Clin Exp Ophthalmol 2016;44:63–64.
11. Gupta MP, Coombs P, Prockop SE, et al. Treatment of cytomegalovirus retinitis with cytomegalovirus-specific T-lymphocyte infusion. Ophthalmic Surg Lasers Imaging Retina 2015; 46:80–82.
12. Brar M, Kozak I, Freeman WR, et al. Vitreoretinal interface abnormalities in healed cytomegalovirus retinitis. Retina 2010; 30:1262–1266.
13. Stevenson W, Prospero Ponce CM, Agarwal DR, et al. Epiretinal membrane: optical coherence tomography-based diagnosis and classification. Clin Ophthalmol 2016;10:527–534.

14. Pang CE, Spaide RF, Freund KP. Epiretinal proliferation seen in association with lamellar macular holes: a distinct clinical entity. Retina 2014;34:1513–1523.
15. Pang CE, Maberley DA, Freund KB, et al. Lamellar hole-associated epiretinal proliferation: a clinicopathologic correlation. Retina 2016;36:1408–1412.
16. Compera D, Entchev E, Haritoglou C, et al. Correlative microscopy of lamellar hole-associated epiretinal proliferation. J Ophthalmol 2015;2015:1–8.
17. Sun JK, Lin MM, Lammer J, et al. Disorganization of the retinal inner layers as predictor of visual acuity in eyes with center-involved diabetic macular edema. JAMA Ophthalmol 2015;132:1309–1316.
18. Wyhinny GJ, Apple DJ, Guastella FR, et al. Adult cytomegalic inclusion retinitis. Am J Ophthalmol 1973;76:773–781.
19. Wilkerson I, Laban J, Mitchell JM, et al. Retinal pericytes and cytomegalovirus infectivity: implications for HCMV-induced retinopathy and congenital ocular disease. J Neuroinflammation 2014;12:1.
20. Zhang M, Xin H, Roon P, et al. Infection of retinal neurons during murine cytomegalovirus retinitis. Invest Ophthalmol Vis Sci 2005;46:2047–2055.
21. Hagiwara A, Mitamura Y, Kumagai K, et al. Photoreceptor impairment on optical coherence tomographic images in patients with retinitis pigmentosa. Br J Ophthalmol 2013;97:237–238.
22. Aizawa S, Mitamura Y, Hagiwara A, et al. Changes of fundus autofluorescence, photoreceptor inner and outer segment junction line, and visual function in patients with retinitis pigmentosa. Clin Exp Ophthalmol 2010;38:597–604.
23. Wakabayashi T, Oshima Y, Fujimoto H, et al. Foveal microstructure and visual acuity after retinal detachment repair: imaging analysis by Fourier-domain optical coherence tomography. Ophthalmology 2009;116:519–528.
24. Bottoni F, De Angelis S, Luccarelli S, et al. The dynamic healing process of idiopathic macular holes after surgical repair: a spectral-domain optical coherence tomography study. Invest Ophthalmol Vis Sci 2011;52:4439–4446.
25. Hartmann KI, Gomez ML, Bartsch DU, et al. Effect of change in drusen evolution on photoreceptor inner segment/outer segment junction. Retina 2012;32:1492–1499.
26. Maheshwary AS, Oster SF, Yuson RM, et al. The association between percent disruption of the photoreceptor inner segment-outer segment junction and visual acuity in diabetic macular edema. Am J Ophthalmol 2010;150:63–67.
27. Theodossiadis PG, Theodossiadis GP, Charonis A, et al. The photoreceptor layer as a prognostic factor for visual acuity in the secondary epiretinal membrane after retinal detachment surgery: imaging analysis by spectral-domain optical coherence tomography. Am J Ophthalmol 2011;151:973–980.
28. Uji A, Murakami T, Nishijima K, et al. Association between hyperreflective foci in the outer retina, status of photoreceptor layer, and visual acuity in diabetic macular edema. Am J Ophthalmol 2012;153:710–717.
29. Yeh S, Forooghian F, Faia L, et al. Fundus autofluoresence changes in cytomegalovirus retinitis. Retina 2010;30:42–54.